



# Experimental study of $ZrB_2-Si_3N_4$ on the microstructure, mechanical and electrical properties of high grade AA8011 metal matrix composites



J. Fayomi <sup>a,\*</sup>, A.P.I. Popoola <sup>a</sup>, O.P. Oladijo <sup>b</sup>, O.M. Popoola <sup>c</sup>, O.S.I. Fayomi <sup>a,d</sup>

<sup>a</sup> Department of Chemical, Metallurgical and Materials Engineering, Tshwane University of Technology, P.M.B. X680, Pretoria, South Africa

<sup>b</sup> Department of Chemical, Materials and Metallurgical Engineering, Botswana International University of Science and Technology, Private Bag 16, Palapye, Botswana

<sup>c</sup> Department of Electrical Engineering, Tshwane University of Technology, P.M.B. X680, Pretoria, South Africa

<sup>d</sup> Department of Mechanical Engineering, Covenant University, P.M.B. 1023, Ota, Nigeria

## ARTICLE INFO

### Article history:

Received 8 February 2019

Received in revised form

5 March 2019

Accepted 6 March 2019

Available online 7 March 2019

### Keywords:

$ZrB_2-Si_3N_4$

Stir casting

AA8011

Aluminium metal matrix composites

Microstructure

Mechanical properties

## ABSTRACT

The present study evaluates the hybrid effect of  $ZrB_2-Si_3N_4$  on the properties of AA8011 metal matrix composites (AMMCs) developed by two steps stir casting process. The percentage of reinforcement varies from 0% to 20% weight. The microstructure, hardness, ultimate tensile strength, yield strength, electrical resistivity, and conductivity were examined. From the results, it was revealed that the mechanical properties of the reinforced alloy are well improved compared to the unreinforced alloy. The optical micrograph and the scanning electron micrograph images with energy dispersive spectroscopy show the uniform distribution of the hybrid particulates of  $ZrB_2-Si_3N_4$  with no visible porosity. The electrical resistivity of the developed AA8011 composites was also improved with the increase in weight percent of the ceramic particulates, but the electrical conductivity was drastically reduced.

© 2019 Elsevier B.V. All rights reserved.

## 1. Introduction

The wide application of aluminium alloy as a primary material in the industry is inestimable due to its high strength-to-light weight ratio, low density, high corrosion resistance, high ductility, availability and affordability [1]. However, some structural challenges like poor tribology, low thermal stability, low hardness, and tensile strength limits its usage or application in most engineering settings [2]. The limitations can be mitigated by reinforcing the soft ductile aluminium alloy with a second discontinuous phase such as hard ceramic (oxides, carbides, borides, and nitrides); to form aluminium metal matrix composite (AMMCs) [3]. AMMCs have been considered globally for use in the automotive, aerospace and architectural sectors because of their superior properties over aluminium alloy [4]. Aluminium metal matrix composites are grossly becoming an inevitable attractive material for advanced

applications in aerospace, automobile, textile, marine, chemical and in general engineering applications.

Particles reinforced metal matrix composites (MMCs) have been the most popular light material over the last few years, with the priority of optimizing the major engineering properties of (AMMCs) [5]. Various methods are in existence to develop the aluminium metal matrix composites, these include stir casting, powder metallurgy, squeeze casting etc. [6]. The type and extent of reinforcement observed, the microstructural degree of integrity desired, dispersed homogenous orientations of reinforcements, cost effect of fabrications, volume percent fractions of production, etc., are some of the major factors that determine the selection of the development process of AMMCs [1,3].

Stir casting is a liquid state fabrication method and one of the most inexpensive and easiest processes for composite manufacturing because of their simplicity, scalability, and high production rate [6,7]. It is widely used for applications that require high production volumes and low cost [8,9]. Some basic priority factors are put into consideration in developing AMMCs through the stir casting process, this includes: achieving uniform or even

\* Corresponding author.

E-mail address: [218749836@tut4life.ac.za](mailto:218749836@tut4life.ac.za) (J. Fayomi).

dispersion of the hard-ceramic material, ensuring wettability between the matrix and the particulates to obtain a good intermetallic bond, and minimizing porosity in the cast metal matrix composite. The achievement of the factors can be attributed to the geometry and position of the mechanical stirrer, the melting temperature, individual properties of the ceramic particulates and the metal matrix substrate in use [10,11].

ZrB<sub>2</sub>-Si<sub>3</sub>N<sub>4</sub> silicon nitride and zirconium diborides are hard ceramic particulates which are characterized by high mechanical strength, excellent thermal stability, high melting point, effective electrical properties, good corrosion and wear behavior [9,11]. Reinforcing Aluminium alloy with ZrB<sub>2</sub>-Si<sub>3</sub>N<sub>4</sub> will improve the properties of the composites. A lot of works has been done on the reinforcement of AMMCs with hard ceramic particulates to improve on the properties of the monolithic alloy. Review from past literature revealed that the reinforcement particulates enhanced the mechanical properties, electrical properties improve corrosion resistance and reduce wear rates [12–14].

However, in the contemporary studies, there is no work done on the mechanical, electrical and microstructure of ZrB<sub>2</sub>-Si<sub>3</sub>N<sub>4</sub> particulates reinforced high grade AA8011 metal matrix composites. Hence, the novelty of this current research is on the hybrid effect of the ZrB<sub>2</sub>-Si<sub>3</sub>N<sub>4</sub> particulate reinforcements on the microstructure, mechanical, and electrical properties of AA8011.

## 2. Materials and methods

### 2.1. Materials

Commercial aluminium AA8011 alloy pellet of purity 97.86% were obtained from aluminium rolling company ota, Nigeria. Zirconium Diboride (ZrB<sub>2</sub>) Nano powder of 99.9% purity, 40–50-nm particle size and Silicon Nitride (Si<sub>3</sub>N<sub>4</sub>) 99.9% purity, 40–50-nm particle size was used in this work. All the powders were supplied by Hongwu International Group, China. The masses of the ceramic powders (ZrB<sub>2</sub> and Si<sub>3</sub>N<sub>4</sub>) were measured in 50:50 wt proportion and mixed to achieve homogenous mixing before admixing with the molten AA8011 see Table 1 and 2.

### 2.2. Methods

#### 2.2.1. Two-step stir casting

The quantity of Aluminium (8011) alloy and ZrB<sub>2</sub>-Si<sub>3</sub>N<sub>4</sub> ceramic particulates required to fabricate composites with 5, 10, 15, and 20 vol percent ZrB<sub>2</sub>-Si<sub>3</sub>N<sub>4</sub> were evaluated by weight proportion. The ceramic particulates were preheated at 450 °C for 10 min to assist remove impurities and break the gas layers present on the surface of the particles. The AA8011 were charged into a graphite crucible furnace and heated to 700 °C (above the melting temperature of the alloy) and the liquid AA8011 was then allowed to cool in the furnace to a semi-solid state at about 650 °C. The preheated ZrB<sub>2</sub>-Si<sub>3</sub>N<sub>4</sub> was added at this temperature and stirring of the slurry was performed manually for 300 s. The composite slurry was then superheated to 800 °C and a second stirring performed using a mechanical stirrer. The stirring operation was performed at a speed of 300 rpm for 300 s to aid in improving the uniform dispersion of the ZrB<sub>2</sub>-Si<sub>3</sub>N<sub>4</sub> particulates in the molten AA8011, improve wettability between the matrix and the particles and the minimum time

**Table 1**  
Chemical composition of the AA8011.

Mg	Si	Mn	Cu	Zn	Ti	Fe	Na	B	Pb	Al
0.47	0.46	0.09	0.14	0.22	0.01	0.61	0.01	0.01	0.01	97.86

**Table 2**  
Percentage composition of the composite admixed.

sample	Al wt.%	ZrB <sub>2</sub> -Si <sub>3</sub> N <sub>4</sub>
A	100	0
B	95	2.5 + 2.5
C	90	5 + 5
D	85	7.5 + 7.5
E	80	10 + 10

of 300 s helps to avoid agglomeration. The molten composite was then cast into prepared sand molds as described by Ref. [6].

#### 2.2.2. Hardness properties

The microhardness of the composites was conducted on Vicker's Microhardness tester (FM-800, Japan) with the 100 g force for the dwelling time of 15s, a spacing of 0.1 with 5 diamond indentation. The dimensioned composite samples of sizes 15 × 15 mm were subjected to grinding and polishing to derive smooth surface finish.

#### 2.2.3. Tensile test

The tensile test was performed using an Instron universal testing machine operated at a constant crosshead speed of 2 mm/s with a 30 kN load. The composites specimen having cross-sectional dimensions of 5 mm by 10 mm with a gauge length of 30 mm were prepared and subjected to the test according to ASTM standards.

#### 2.2.4. Electrical conductivity and resistivity test

The electrical conductivity and resistivity test were performed using a four-point probe meter (HP2662, China) that measure the resistivity of light metals. Test samples with dimensions of 10 mm by 10 mm with a thickness of 1.5 mm were prepared. The current source was set at 100 mA and at a speed of seven times/min. The resistivities were got and converted to conductivities by finding the inverse [15].

#### 2.2.5. Optical microscope (OPM) and scanning electron microscope (SEM)

The samples for microstructural investigation using an OPM and SEM are subjected to metallographic treatment by grinding, polishing and then etched with Keller's reagent to reveal the grain boundaries and remove impurities. The optical microstructural investigation was performed using digital light metallurgical Microscope. TESCAN was used to investigate the structural properties of the developed alloy.

## 3. Results and discussion

### 3.1. Study of mechanical properties of AA8011

#### 3.1.1. Hardness properties

The microhardness of AA8011/ZrB<sub>2</sub>-Si<sub>3</sub>N<sub>4</sub> composites was shown in Fig. 1. From this result, it was obvious that the composites with 20% weight particulate have the highest hardness value due to the hybrid strengthening effect and volume proportion of the ceramic boride and nitride present in the composite alloy. It is evident that hardness increases with an increase in the volume fraction of the hybrid ZrB<sub>2</sub>-Si<sub>3</sub>N<sub>4</sub> particulates. The hybrid particles of ZrB<sub>2</sub>-Si<sub>3</sub>N<sub>4</sub> acted at a point as heterogeneous nucleation in the melt pool of AA8011 matrix, which often resulted in grain refinement and hardener in the matrix as attested by Ref. [16]. No doubt, the hardness enhancement can be attributed to the intrinsic ceramic properties of ZrB<sub>2</sub>-Si<sub>3</sub>N<sub>4</sub> hybrids present in the matrix which tends to increase the load bearing capacity of the (AA8011/ZrB<sub>2</sub>-Si<sub>3</sub>N<sub>4</sub>) composite, as against the primary material (AA8011).

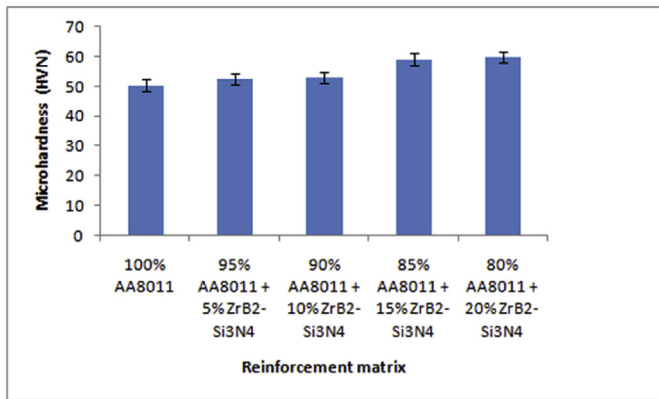


Fig. 1. Progression of Microhardness Properties of Reinforced AA8011 alloy.

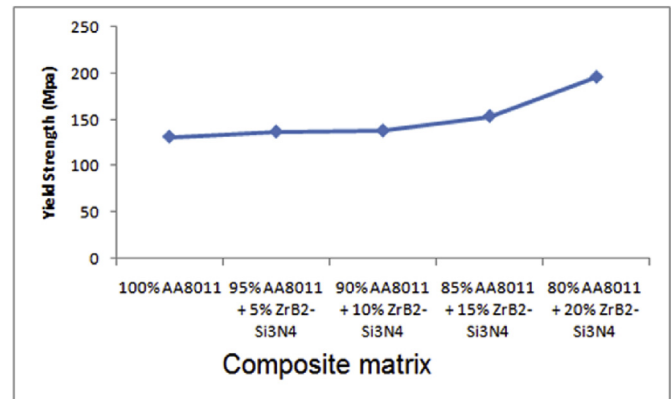


Fig. 3. Progression of Yield Strength of Reinforced AA8011 alloy.

Also, the strong intermetallic bonding that exists between the hybrid particulates and AA8011 because of the complete wettability and homogeneity of the hybrid particulates in the ductile AA8011 could be responsible for the strengthening mechanism [10,12,19].

### 3.1.2. Ultimate tensile strength and yield strength

In Figs. 2 and 3, the results from tensile analysis signify an improvement in the ultimate tensile strength and the yield strength of the composite materials when compared to the as-received samples. It is evident from the results that an improved strength in the case of AMM composites with an increase in hybrid particulate addition is observed both in terms of the strengthening properties described by Ref. [18]. Figs. 2 and 3 shows the variation of ultimate tensile strength (UTS) and the yield strength (YS) of AMMCs when reinforced with 5, 10, 15 and 20 wt % of ZrB<sub>2</sub>-Si<sub>3</sub>N<sub>4</sub> particulates. The ultimate tensile strength and the yield strength of AA8011- ZrB<sub>2</sub>-Si<sub>3</sub>N<sub>4</sub> composite material increases in relative to the AA8011. A noticeable increase in strength is well obtained in 20% wt. of ZrB<sub>2</sub>-Si<sub>3</sub>N<sub>4</sub> as revealed in Figs. 2 and 3. In general, the strengthening mechanism of the mechanical properties can be ascribed to the presence of hard ceramic particles (ZrB<sub>2</sub>-Si<sub>3</sub>N<sub>4</sub>) acting as the restriction to the movement of dislocation due to the increased stress concentration near the matrix-reinforcement interface [10,18]. The increase in strength may also be attributed to the closed packing of particulates within the ductile aluminium alloy AA8011 as a result of improved wettability [17].

The characteristics of aluminium metal matrix composites depend on the individual interfacial properties of the matrix and the reinforcements and these properties further depend on the

intermetallic bonding and adhesion because of complete wettability between the matrix and the particulates constituents. Good bonding between reinforcement and aluminium alloy causes improved strengthening properties of the composites which is in line with the study by Ref. [14].

### 3.2. Evaluation of electrical properties

Fig. 4 shows the results of electrical conductivity and resistivity of the developed composite alloy. From the results, the electrical conductivity decreases with increase in volume percent of the reinforcement. This decrease in electrical conductivity and an increase in resistivity could be attributed to the low conductive nature of particulates and the slight porosity that occur during the fabrication process. The result agrees with the work presented by Refs. [10,20]. In general, the electrical resistivity increases with an increase in weight percentage of ZrB<sub>2</sub>-Si<sub>3</sub>N<sub>4</sub>. Nevertheless, the material with lower electrical conductivity can find their usage in weight sensitive applications like cooking utensils and foils [10,21] (see Fig. 5).

### 3.3. Microstructural studies

The optical micrograph of the developed AA8011/ZrB<sub>2</sub>-Si<sub>3</sub>N<sub>4</sub> composites is shown in Fig. 6a–e with ZrB<sub>2</sub>-Si<sub>3</sub>N<sub>4</sub> particles homogeneously distributed at the interface. The filler concentration of the particulates increases with increase in weight percent of the ZrB<sub>2</sub>-Si<sub>3</sub>N<sub>4</sub> (5%, 10%, 15% and 20%) as seen in Fig. 6a–e. This attests to the efficiency of the two-steps liquid metallurgy technique used in

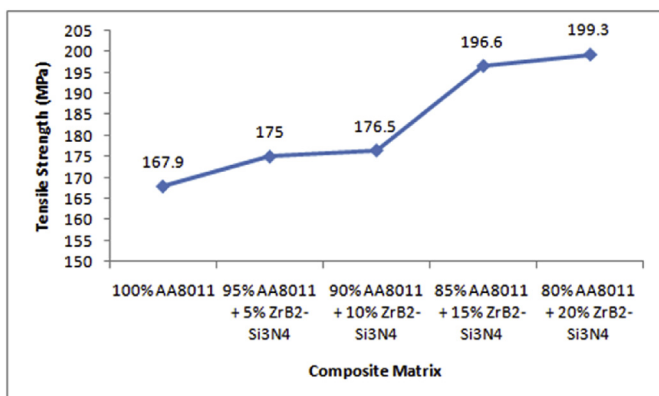


Fig. 2. Progression of Ultimate tensile strength of Reinforced AA8011 alloy.

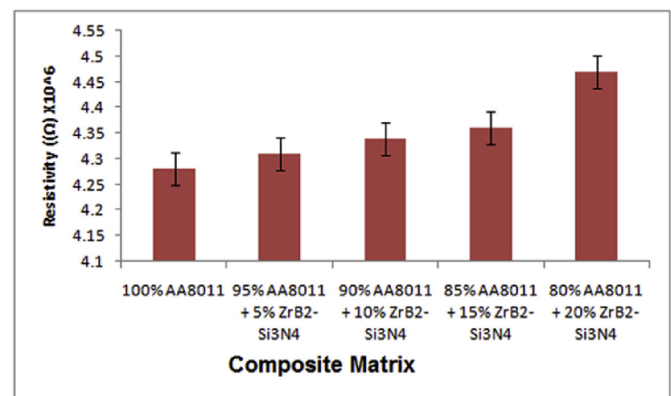


Fig. 4. Trend of electrical resistivity properties of the developed composite alloys.

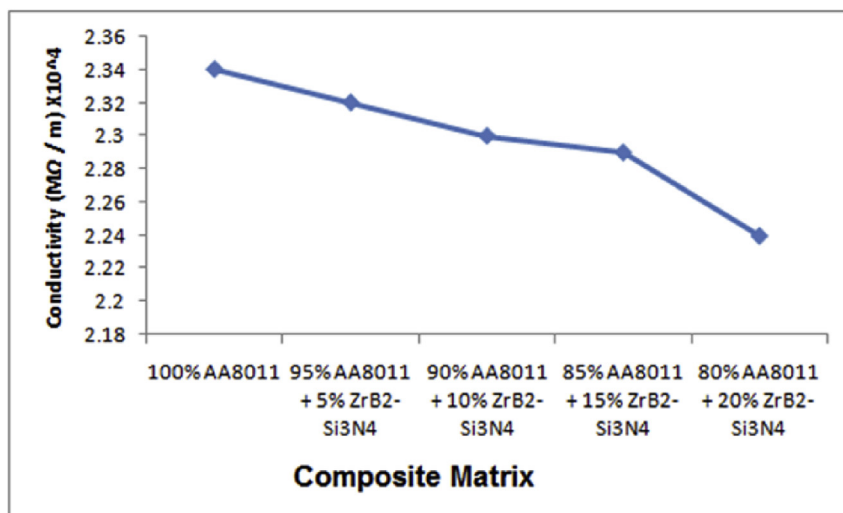


Fig. 5. Trend of electrical conductivity properties of the developed composite alloys.

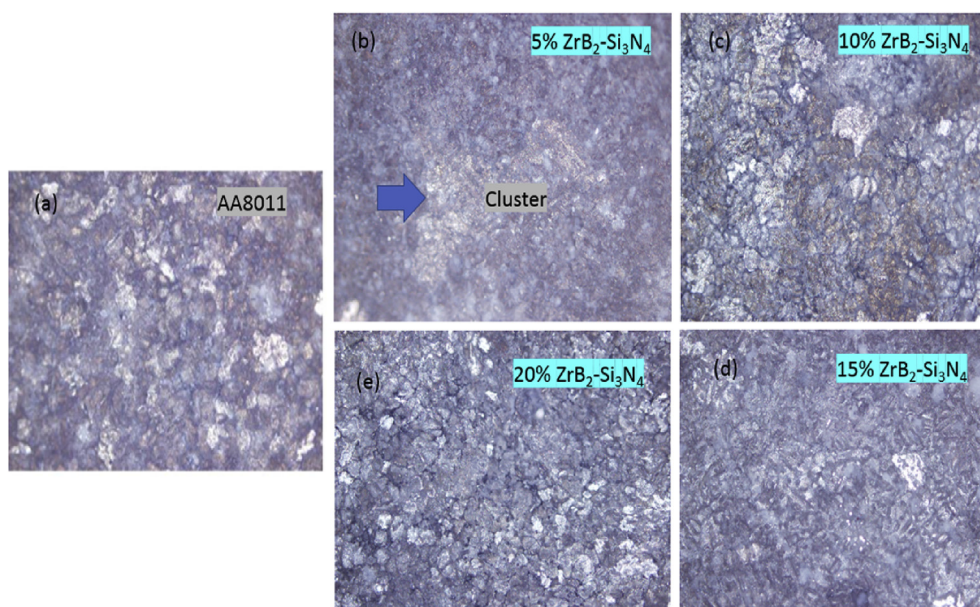


Fig. 6. Optical micrographs of (a) AA 8011 (b) AA 8011 - 5% ZrB<sub>2</sub>-Si<sub>3</sub>N<sub>4</sub>, (c) AA 8011 -10% ZrB<sub>2</sub>-Si<sub>3</sub>N<sub>4</sub>(d) AA 8011-15% ZrB<sub>2</sub>-Si<sub>3</sub>N<sub>4</sub> (e) AA 8011 -20% ZrB<sub>2</sub>-Si<sub>3</sub>N<sub>4</sub>.

developing the composite materials [3,13,22]. Fig. 6a shows the micrograph of the as-received AA8011, it is evident that the entire grey region represents the matrix without reinforcement. As the particulate of ZrB<sub>2</sub>-Si<sub>3</sub>N<sub>4</sub> is consolidated into the melt pool of the molten metal (AA8011), whitish region was observed which depict the present of a foreign ceramic material (ZrB<sub>2</sub>-Si<sub>3</sub>N<sub>4</sub>) embedded in the base matrix shown in Fig. 6b–e it is worthy of note that as the volume fraction of the particulate increases from 5% to 20%, the whitish region becomes heavy and well dispersed uniformly. The optical micrograph shows vividly the uniform dispersion of the particulates, with small clustering observed in material reinforced with 5% ZrB<sub>2</sub>-Si<sub>3</sub>N<sub>4</sub> as shown in Fig. 6b this small agglomeration inform of clustering observed at 5% percent weight of ZrB<sub>2</sub>-Si<sub>3</sub>N<sub>4</sub> might be due to the stirring process, but in all there was a strong interfacial bonding between the ZrB<sub>2</sub>-Si<sub>3</sub>N<sub>4</sub> particles and aluminium metal matrix (AA8011). The strong intermetallic bonding, excellent wettability between the continuous metal phase

and the discontinuous reinforcement phase, and the uniform distribution can be attributed to the process parameters used through two steps stir casting route [1,13].

The SEM micrograph in Fig. 7a–e revealed the microstructure of the base matrix AA8011 and the hybrid composite samples containing 5%, 10%, 15% and 20% volume fraction of ZrB<sub>2</sub>-Si<sub>3</sub>N<sub>4</sub>. The micrographs clearly show no visible micro-cracks and small clustering of particulates within the matrix. The distribution of the hybrid reinforcements in each of the micrographs clearly indicate uniformity that is, homogeneity of particulates within the ductile matrix and this can be attributed to the process parameters via two steps stir casting route [18]. In Fig. 7e, the micrograph shows that the matrix is made up of aluminium specifically AA8011 without any reinforcement. This is evident from the EDS spectra display in Fig. 7f which indicated the major constituents of AA8011 (Al, Si, and Fe). Fig. 7d clearly indicate an even dispersion of hybrid reinforcement in form of granular grains though sparsely distributed



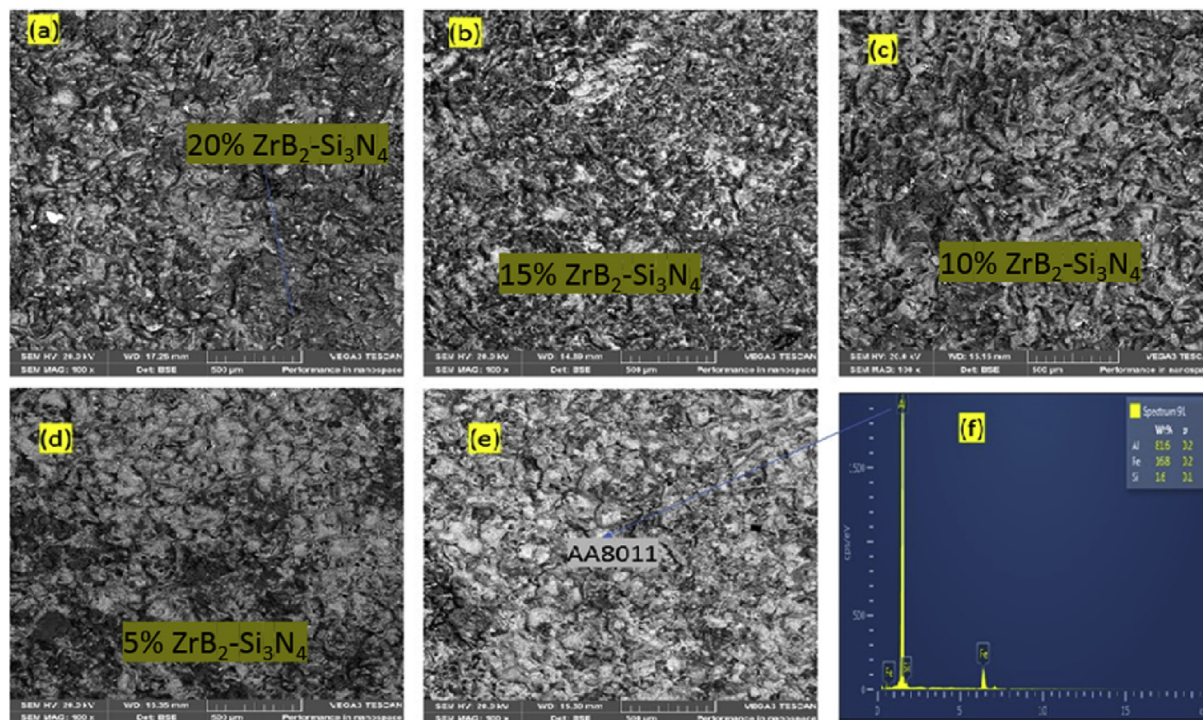


Fig. 7. SEM micrographs of (a) AA 8011 - 20%  $ZrB_2-Si_3N_4$  (b) AA 8011-15%  $ZrB_2-Si_3N_4$  (c) AA 8011-10%  $ZrB_2-Si_3N_4$  (d) AA 8011-5%  $ZrB_2-Si_3N_4$  (e) AA 8011 (f) EDX AA8011.

due to the volume fraction in the matrix (5%). But in Fig. 7c, b, and a, the grey-dark fillers were observed to be heavy and uniformly distributed in the ductile matrix with no pore space thereby enhancing the properties of the composite alloy. The grain refinements of the second discontinuous phase precipitates were clearly revealed along the grain boundaries with the increase in the weight percent of the particulates. Therefore, it is not out of context if stated that the two steps stir casting process parameters which encompass preheating of the hybrid particulates to degas the surface layer against air entrapment, the stirring speed before and after mixing of matrix with particulates, and the stirring time is responsible for the homogenous dispersion of the reinforcement with no void microcracks [18]. Moreso, clustering, segregation, and agglomeration could also influence intermetallic bonding along the grain boundaries due to complete wettability [22].

#### 4. Conclusion

The following conclusions were derived:

AA8011-  $ZrB_2-Si_3N_4$  composites have been successfully developed.

- The Fabrication of aluminum base composites using two-step stir casting process route results in uniform distribution of the discontinuous reinforcement phase ( $ZrB_2-Si_3N_4$ ).
- The mechanical properties of AMMCs composites increased with increase in weight percent fraction of reinforcements.
- The mechanical strength of AA8011-20 vol %  $ZrB_2-Si_3N_4$  composite is superior to those of the 5, 10 and 15 wt % AA8011- $ZrB_2$  matrix composite materials.
- The resistivity of the developed AMMCs was enhanced with an increasing percentage volume of the particulates. Whereas the electrical conductivity decreases with increase in reinforcement.

#### Acknowledgments

The author will like to acknowledge the support from Department of Chemical, Metallurgical and Material Engineering, Tshwane University of Technology Pretoria South Africa.

#### References

- [1] A.O. Inegbemor, C.A. Bolu, P.O. Babalola, A.I. Inegbemor, O.S.I. Fayomi, Aluminum Silicon Carbide Particulate Metal Matrix Composite Development via Stir Casting Processing, Springer Science Business Media Dordrecht, 2016. JrnllD 12633 ArtID 9451.
- [2] G.R. Jinu, G. Karthikeyan, P. Vijayalakshmi, Development and mechanical properties analysis of aluminum LM14- mgo metal matrix composite using FEA, *Concurr. Adv. Mech. Eng.* 2 (2) (2016) 20–32.
- [3] P.O. Babalola, A.O. Inegbemor, C.A. Bolu, A.I. Inegbemor, The development of molecular based materials for electrical and electronic application, *J. Miner. Met. Miner. Soc. (TMS)* 67 (4) (2015) 830–834.
- [4] O.S.I. Fayomi, M. Abdulwahab, S.A. Yaro, F. Asuke, A.O. Inegbemor, A. Kasim, Effect of multifunctional composite infringement on the electrochemical propagation and characterization of al-mg-si/tio2-sno2 composite by stir casting method, *J. Adv. Electrochem.* 1 (1) (2015) 9–12.
- [5] N. Prasad, Development and Characterization of Metal Matrix Composite Using Red Mud an Industrial Waste for Wear Resistant Applications, *Thesis National Institute of Technology Rourkela-769008*, (Orissa), India, 2006, p. 5.
- [6] K.K. Alaneme, M.O. Bodunrin, Mechanical behavior of alumina reinforced aa 6063 metal matrix composites developed by two steps – stir casting process, *Acta Technica Corviniensis Bull. Eng.* (2013). ISSN: 2067-3809.
- [7] M. Kok, Production and mechanical properties of  $Al_2O_3$  particle reinforced 2024 Aluminium composites, *J. Mater. Process. Technol.* 16 (2005) 381–387.
- [8] B.A. Kumar, N. Murugan, *Composite Mat. Des.* 40 (2012) 52–58.
- [9] S.S. Prem, R. Banchhor, Fabrication methods used to prepare Al metal matrix composites- A review, *Int. Res. J. Eng. Technol. (IRJET)* 03 (10) (2016).
- [10] J. Michael, J.S. Kumar, Fabrication and Characterization of hybrid aluminium metal matrix composite, *Int. Res. J. Eng. Technol. (IRJET)* 05 (06) (2018).
- [11] P. Sharma, S. Sharma, D. Khanduja, Production and some properties of  $Si_3N_4$  reinforced aluminium alloy composites, *J. Asian Ceram. Soc.* 3 (2015) 352–359.
- [12] R.J. Kandan, D. Kumar, M. Sudharssanam, Venkadesan, R. Badrinath, Investigation of mechanical properties on newly formulated hybrid composite aluminium 8011 reinforced with B4C and  $Al_2O_3$  by stir casting method, *Int. J. Sci. Res. develop.* 5 (issue 01) (2017).
- [13] A.P.I. Popoola, S.L. Pityana, O.M. Popoola, Microstructure and corrosion properties of Al (Ni/TiB<sub>2</sub>) intermetallic matrix composite coatings, *J. South.*

- Afr. Inst. Min. Metall. 111 (2011) 345. SA ISSN 0038–223X/3.00.
- [14] H.K. Shivanand, A. Yogananda, Development and characterization of corrosion properties of aluminium 8011 hybrid metal matrix composites, in: Proceedings of 9th IRF International Conference, 2015, ISBN 978-93-82702-93-1.
- [15] C.O. Ujah, A.P.I. Popoola, O.M. Popoola, V.S. Aigbodion, Electrical conductivity, mechanical strength and corrosion characteristics of spark plasma sintered Al-Nb nanocomposite, *Int. J. Adv. Manuf. Technol.* (2018). <https://doi.org/10.1007/s00170-018-3128-x>.
- [16] V.R. Rao, N. Ramanaiah, Sarcar, Dry sliding wear behavior of Tic –AA7075 metal matrix composites, *Int. J. Appl. Sci. Eng.* 1 (2016) 27–37.
- [17] D. Ramesh, R.P. Swamy, T.K. Chandrashekar, Effect of weight percentage on mechanical properties of frit particulate reinforced al6061 composite, *ARPN J. Eng. Appl. Sci.* 5 (1) (2010) 1819–6608.
- [18] R. Karthigeyan, G. Ranganath, S. Sankaranarayanan, Mechanical properties and microstructure studies of aluminium (7075) alloy matrix composite reinforced with short basalt fibre, *Euro. J. Sci. Res.* 68 (No.4) (2012) 606–615. ISSN 1450-216X.
- [19] B. Ravi, Fabrication and mechanical properties of Al7075-sic-tic hybrid metal matrix composites, *Int. J. Eng. Sci. Invent.* 6 (10) (2017) 12–19. ISSN (Online): 2319 – 6734, [www.ijesi.org](http://www.ijesi.org).
- [20] M.M.M. Mohammed, O.A. Elkady, A.W. Abdelhameed, Effect of alumina particles addition on physico-mechanical properties of Al-matrix composites, *Open J. Met.* 3 (2013) 72–79.
- [21] E.A. Starke JR, H.M.M.A. Rashed, Alloys: aluminium, *Ref. Modul. Mater. Sci. Mater. Eng.* (2017), <https://doi.org/10.1016/B978-0-12-803581-8.09210-9>: 1-8 (Elsevier).
- [22] N. Muralidharan, K. Chockalingam, I. Dinaharan, K. Kalaiselvan, Microstructure and mechanical behaviour of AA2024 aluminium composites reinforced with in-situ synthesized Zr<sub>2</sub> particles, *J. Alloys Compd.* 735 (2018) 2167–2174.